Inorg. Chem. **2004**, *43*, 3151–3158

Electron Delocalization in Nickel Metallic Wires: A DFT Investigation of $Ni_3(dpa)_4Cl_2$ and $[Ni_3(dpa)_4]^{3+}$ (dpa = Dipyridylamide) and Extension to Higher Nuclearity Chains

Pascal Kiehl, Marie-Madeleine Rohmer, and Marc Bénard*

Laboratoire de Chimie Quantique, UMR 7551, CNRS and Université Louis Pasteur, 4 rue Blaise Pascal, F-67000 Strasbourg, France

Received January 26, 2004

The electronic structure of $Ni_3(dpa)_4Cl_2$ (**1**) has been investigated within the framework of the density functional theory (DFT), using two types of exchange-correlation functionals and various basis sets. The "broken-symmetry" approach proposed by Noodleman for the characterization of electronic states displaying an antiferromagnetic coupling has been applied to **1**. All calculations lead to the conclusion that the ground state results from an antiferromagnetic coupling between the terminal Ni atoms, both displaying a high-spin electronic configuration. The central Ni atom is in a low-spin configuration, but is involved in a superexchange interaction connecting the two magnetic centers. These results are in agreement with the assignments recently proposed by the group of F. A. Cotton on the basis of magnetic measurements. It is shown that the ground state electronic configuration calculated for **1** provides the trinickel framework with some delocalized σ bonding character. The observed geometry of **1** is accurately reproduced by the broken-symmetry solution. The doublet ground state assigned to the oxidized species $[Ni_3(dpa)_4]^{3+}$ (**2**) and the dramatic contraction of the coordination sphere of the terminal metals observed upon oxidation are also confirmed by the calculations. However, the *formal* Ni–Ni bond order is not expected to increase in the oxidized species. The contraction of the Ni–Ni distance in **2** is shown to result in part from the vanishing of the important *trans* influence originating in the axial ligands, and for the rest from a more efficient shielding of the metal nuclear charge along the Ni–Ni–Ni axis. The conclusions deduced from the analysis of the bonding in **1** and **2** can be extended to their homologues with higher nuclearity. More specifically, it is predicted that the single occupancy of the most antibonding σ orbital, extending over the whole metal framework, will provide the $(Ni_p)^{2p/(2p+1)+}$ chains with some delocalized bonding character and, possibly, with electrical conduction properties.

Introduction

The quest for materials associated with unusual electrical, optical, magnetic, or superconducting properties has been since several decades an incentive toward the characterization of low dimensional compounds organized around linear chains of interacting metal atoms.[1] More recently, the growing interest in the specific properties of nanoscale materials has stirred the attention toward the synthesis, the characterization and the fine-tuning of discrete clusters in which a variable number of metal atoms, larger than two and presently limited to nine,[2] retain a linear conformation. These families of linear clusters have been recently reviewed by Bera and Dunbar, who divide them into two classes, depending on the linear conformation being either obtained through unsupported metal−metal interactions or constrained by the polydentate ligand environment of the metal framework.[3] Two groups of ligands have presently been investigated in relation to their propensity to stabilize chains of metal atoms, namely, the conjugated polyenes[4] and the polypyridylamide anions, which are *p*-dentate ligands with general formula $[C_5H_4N-N-(C_5H_3N-N)_n-C_5H_4N]^{(n+1)-}$ and $p = 2n + 3$. These ligands appear particularly promising and versatile in many respects. They could be extended and

* Corresponding author. Tel: 33 390 241 301. Fax: 33 390 241 589. E-mail: benard@quantix.u-strasbg.fr.

(1) *Extended Linear Chain Compounds*; Miller, J. S., Ed.; Plenum: New York, 1982.
(2) Peng, S.-M., Wang, C.-C.; Jang, Y.-L.; Chen, Y.-H., Li, F.-Y., Mou, C.-Y., Leung, M.-K. *J. Magn. Magn. Mater.* **2000**, *209*, 80.
(3) Bera, J. K.; Dunbar, K. R. *Angew. Chem., Int. Ed.* **2002**, *41*, 4453.
(4) Murahashi, T., Nagai, T., Mino, Y., Mochizuki, E., Kai, Y., Kurosawa, H. *J. Am. Chem. Soc.* **2001**, *123*, 6927.

10.1021/ic040011j CCC: $27.50
Published on Web 04/15/2004

controlled in order to synthesize what is to our knowledge the discrete cluster with largest linear metal backbone, $Ni_9(\mu_9\text{-peptea})_4Cl_2$, with peptea = pentapyridyltetramide ($n = 3$).[2] While the longest metal strings synthesized with this family of ligands have been obtained with nickel and chromium only,[2] the prototypical members of this class of clusters, namely, the trinuclear complexes $M_3(\mu_3\text{-dpa})_4XY$ (dpa = dipyridylamide, $n = 0$; X, Y being axial anionic ligands) were characterized with a large variety of transition metals, namely, Cr, Ru, Co, Rh, Ni, Cu.[5] An elaborate chemistry has also been focused on the properties of the terminal ligands.[6] Comprehensive studies carried out in the group of F. A. Cotton on the trinuclear complexes of cobalt[5f,g,7] and chromium[5h,i,8] have evidenced an unprecedented structural instability that could be tentatively assigned to the competition between different types of spin coupling within the metal framework.[9] As emphasized by Cotton et al., the correct knowledge of the molecular structure conditions the understanding of the electronic structure,[10] which itself determines a key property of molecular wires, namely, the localization or delocalization of the metal electrons and the electrical conduction.[10,12,13] Indeed, the intuitive idea that electrical conduction along a linear molecule is enhanced by electron delocalization and hampered by bond length alternation has recently received support from experiment and theory.[11] The goal of the present paper is to discuss the localization/delocalization issue via DFT calculations on $Ni_3(dpa)_4Cl_2$ (**1**) and on the oxidized cluster $[Ni_3(dpa)_4]^{3+}$ (**2**) (Figure 1), which are both structurally well characterized.[5c,12−15] Indeed, the spectacular contraction of the coordination sphere observed around the terminal Ni atoms in **2** has been interpreted in terms of a bonding interaction delocalized along the $(Ni_3)^{7+}$ framework, and opposed to the localized electronic structure assumed for the $(Ni_3)^{6+}$ species.[13−15] Furthermore, it has been recently shown that the shortening of the Ni−Ni distances upon oxidation spreads over the whole metal chain in $(Ni_5)^{11+}$ complexes.[16,17] An extrapolation of these structural and electronic trends to the higher homologues of the $(Ni_p)^{(2p+1)+}$ series has been attempted, opening the way toward the tuning of nanoscale conductive wires.[17] However, the real origin and nature of the electron reorganization and of the structural changes observed upon oxidation have, to our knowledge, never been clearly established.[13−15] The calculations reported here show that the change in axial coordination has also to be taken into consideration and that the distinction between "localized" $(Ni_p)^{2p+}$ and "delocalized" $(Ni_p)^{(2p+1)+}$ clusters may not be so clear-cut as previously assumed.[13−15,17]

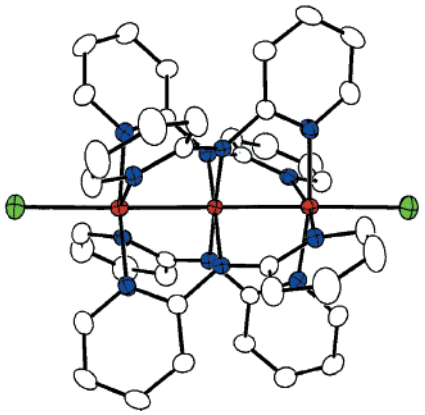

Figure 1. Observed structure of $Ni_3(dpa)_4Cl_2$: Ni, red; Cl, green; N, blue; C, white.

Computational Details

Calculations and geometry optimizations have been carried out using the formalism of the density functional theory (DFT). Two types of exchange-correlation functionals have been used: (i) the so-called Becke-Perdew/86 (BP86) functional,[18] which belongs to the family of functionals referring to the generalized gradient approximation (GGA), and (ii) the B3LYP functional,[19] prototypical of the "hybrid" Hartree−Fock/GGA exchange functionals. Calculations using BP86 have been carried out with the 1999 release of

(5) (a) Wu, L.-P.; Field, P.; Morrissey, T.; Murphy, C.; Nagle, P.; Hathaway, B.; Simmons, C.; Thornton, P. *J. Chem. Soc., Dalton Trans.* **1990**, 3835. (b) Pyrka, G. J.; El-Mekki, M.; Pinkerton, A. A. *J. Chem. Soc., Chem. Commun.* **1991**, 84. (c) Aduldecha, S.; Hathaway, B. *J. Chem. Soc., Dalton Trans.* **1991**, 993. (d) Sheu, J.-T.; Lin, C.-C.; Chao, I.; Wang, C.-C.; Peng, S.-M. *Chem. Commun.* **1996**, 315. (e) Yang, E.-C.; Cheng, M. C.; Tsai, M.-S.; Peng, S.-M. *J. Chem. Soc., Chem. Commun.* **1994**, 2377. (f) Cotton, F. A.; Daniels, L. M.; Jordan, G. T., IV. *Chem. Commun.* **1997**, 421. (g) Cotton, F. A.; Daniels, L. M.; Jordan, G. T., IV; Murillo, C. A. *J. Am. Chem. Soc.* **1997**, *119*, 10377. (h) Cotton, F. A.; Daniels, L. M.; Murillo, C. A.; Pascual, I. *J. Am. Chem. Soc.* **1997**, *119*, 10233. (i) Cotton, F. A.; Daniels, L. M.; Murillo, C. A.; Pascual, I. *Inorg. Chem. Commun.* **1998**, *1*, 1.

(6) (a) Tsao, T.-B.; Lee, G.-S.; Yeh, C.-H.; Peng, S.-M. *Dalton Trans.* **2003**, 1465. (b) Sheng, T.; Appelt, R.; Comte, V.; Vahrenkamp, H. *Eur. J. Inorg. Chem.* **2003**, 3731.

(7) (a) Clérac, R.; Cotton, F. A.; Daniels, L. M.; Dunbar, K. R.; Kirschbaum, K.; Murillo, C. A.; Pinkerton, A. A.; Schultz, A. J.; Wang, X. *J. Am. Chem. Soc.* **2000**, *122*, 6226. (b) Clérac, R.; Cotton, F. A.; Daniels, L. M.; Dunbar, K. R.; Murillo, C. *J. Chem. Soc., Dalton Trans.* **2001**, 386. (c) Clérac, R.; Cotton, F. A.; Daniels, L. M.; Dunbar, K. R.; Murillo, C. *Inorg. Chem.* **2001**, *40*, 1256. (d) Clérac, R.; Cotton, F. A.; Jeffery, S. P.; Murillo, C. A.; Wang, X. *Inorg. Chem.* **2001**, *40*, 1265. (e) Berry, J. F.; Cotton, F. A.; Lu, T.; Murillo, C. A. *Inorg. Chem.* **2003**, *42*, 4425.

(8) (a) Cotton, F. A.; Daniels, L. M.; Murillo, C. A.; Wang, X. *Chem. Commun.* **1998**, 39. (b) Clérac, R.; Cotton, F. A.; Daniels, L. M.; Dunbar, K. R.; Murillo, C. A.; Pascual, I. *Inorg. Chem.* **2000**, *39*, 748, 752. (c) Cotton, F. A.; Lei, P.; Murillo, C. A. *Inorg. Chim. Acta* **2003**, *349*, 173. (d) Cotton, F. A.; Lei, P.; Murillo, C. A.; Wang, L. S. *Inorg. Chim. Acta* **2003**, *349*, 165.

(9) (a) Rohmer, M.-M., Bénard, M. *J. Am. Chem. Soc.* **1998**, *120*, 9372. (b) Rohmer, M.-M., Strich, A.; Bénard, M.; Malrieu, J.-P. *J. Am. Chem. Soc.* **2001**, *123*, 9126. (c) Benbellat, N.; Rohmer, M.-M., Bénard, M. *Chem. Commun.* **2001**, 2368.

(10) (a) Cotton, F. A.; Daniels, L. M.; Murillo, C. A.; Wang, X. *Chem. Commun.* **1999**, 2461. (b) Cotton, F. A.; Daniels, L. M.; Lu, T.; Murillo, C. A.; Wang, X. *J. Chem. Soc., Dalton Trans.* **1999**, 517.

(11) (a) Paul, F.; Lapinte, C. *Coord. Chem. Rev.* **1998**, *178−180*, 431 and references therein. (b) Joachim, C.; Launay, J. P.; Woitellier, S. *Chem. Phys.* **1990**, *147*, 131.

(12) Clérac, R.; Cotton, F. A.; Dunbar, K. R.; Murillo, C. A.; Pascual, I.; Wang, X. *Inorg. Chem.* **1999**, *38*, 2655.

(13) Berry, J. F.; Cotton, F. A.; Daniels, L. M.; Murillo, C. A. *J. Am. Chem. Soc.* **2002**, *124*, 3212.

(14) Berry, J. F.; Cotton, F. A.; Daniels, L. M.; Murillo, C. A.; Wang, X. *Inorg. Chem.* **2003**, *42*, 2418.

(15) Berry, J. F.; Cotton, F. A.; Lu, T.; Murillo, C. A.; Wang, X. *Inorg. Chem.* **2003**, *42*, 3595.

(16) Yeh, C. Y.; Chiang, Y.-L.; Lee, G.-H.; Peng, S.-M. *Inorg. Chem.* **2002**, *41*, 4096.

(17) Berry, J. F.; Cotton, F. A.; Lei, P.; Lu, T.; Murillo, C. A. *Inorg. Chem.* **2003**, *42*, 3534.

(18) (a) Becke, A. D. *Phys. Rev.* **1988**, *A38*, 3098. (b) Perdew, J. P. *Phys. Rev.* **1986**, *B33*, 8882; **1986**, *B34*, 7406.

(19) (a) Becke, A. D. *J. Chem. Phys.* **1993**, *98*, 5648. (b) Lee, C.; Yang, W.; Parr, R. G. *Phys. Rev. B* **1988**, *37*, 785.

the ADF program[20] based upon the use of Slater basis sets.[21] The basis sets used in the present calculations are referred to as II in the ADF User's Guide and will be designated as S/II. For first row atoms, the 1s shell was frozen and described by a single Slater function. The neon core of Cl and Ni atoms was also modeled by a minimal, frozen Slater basis. For hydrogen, carbon, nitrogen, and chlorine, the valence-shell was described by a double-ζ Slater basis set. For Ni, the 3s, 3p, and 4s shells are double-ζ, whereas the 3d shell is triple-ζ, and the 4p shell is described by a single orbital. No polarization functions were added. For some calculations a more extended Slater basis set was used (basis set S/IV), which is of triple-ζ quality for the valence shells and includes polarization functions for all atoms, including metals.

Calculations using B3LYP have been carried out with Gaussian 98.[22] Two Gaussian basis sets have been used for these calculations. The first one, referred to as G/I in the present work, consists of using the LANL2DZ bases for the metal atoms and for their coordination shell, namely, for the N and Cl atoms. The carbon and hydrogen atoms are described with the all-electron LANL2MB minimal basis set. The second basis set (G/II) is the same as G/I, except that each LANL2DZ atomic basis has been supplemented with one appropriate d- or f-type polarization function. Calculations on the open-shell states have been carried out using the unrestricted formalism. The antiferromagnetic singlet state of $Ni_3(dpa)_4Cl_2$ has been characterized and its geometry optimized using the broken-symmetry (BS) formalism first proposed by Ginsberg,[23] standardized by Noodleman,[24] discussed and currently used by others.[25−29] The coupling constant $2J_{ab}$ between two magnetic centers a and b is defined as follows by the Heisenberg−Dirac−van Vleck (HDVV) Hamiltonian:[30]

$$\hat{H}^{HDVV} = -2J_{ab}\hat{S}_a\cdot\hat{S}_b \qquad (1)$$

However, a reliable evaluation of $2J_{ab}$ from the energies of the state of maximal spin ^{HS}E and of the broken-symmetry solution ^{BS}E is a nontrivial problem, mainly due to the assumption that ought to be done concerning the overlap between the magnetic orbitals.[31] Yamaguchi et al. have proposed an elegant, though approximate spin projection procedure[32] in which the dependence of $2J_{ab}$ upon the overlap is replaced by a dependence upon the spin contamination of the broken-symmetry solution:

$$2J_{ab} = 2(^{BS}E - {}^{HS}E)/(^{HS}\langle S^2\rangle - {}^{BS}\langle S^2\rangle) \qquad (2)$$

$^{HS}\langle S^2\rangle$ and $^{BS}\langle S^2\rangle$ denoting the spin eigenvalues calculated in the high-spin and in the broken-symmetry solutions, respectively. $^{BS}\langle S^2\rangle$ can in principle vary from zero to S_{max}, where S_{max} represents the maximal spin value. $^{BS}\langle S^2\rangle = 0$ corresponds to the ideal case of a perfect overlap between the magnetic centers, whereas $^{BS}\langle S^2\rangle \sim S_{max}$ indicates a negligible overlap.[32] The spin eigenvalues are provided by Gaussian 98, but unfortunately not by ADF.

Most geometry optimizations have been carried out assuming the symmetry constraints of either the D_4, or—for the broken-symmetry calculations—of the C_4 symmetry point groups. The C_2 or the D_2 subgroups have been used in some cases, without any significant deviation from ideal symmetry.

$Ni_3(dpa)_4Cl_2$ in a Delocalized Orbital Model

The $(Ni_3)^{6+}$ core of the complex is an electron-crowded system with 24 valence electrons. These electrons are distributed among the 15 orbital combinations stemming from the d-type orbitals of individual atoms. The *z* axis is assumed collinear with the Cl−Ni_3−Cl line, so that σ-type MOs are made of d_{z^2} combinations, π and δ MOs being generated from the other d-type atomic orbitals with appropriate orientation.[33] In terms of molecular orbitals symmetry-adapted to the D_4 point group, each type of atomic orbital generates three MOs with bonding, nonbonding (nb), and antibonding character, respectively. The three MOs with σ

(20) (a) *User's Guide, Release 1999;* Chemistry Department, Vrije Universiteit: Amsterdam, The Netherlands, 1999. (b) Baerends, E. J.; Ellis, D. E.; Ros, P. *Chem. Phys.* **1973**, *2*, 41. (c) te Velde, G.; Baerends, E. J. *J. Comput. Phys.* **1992**, *99*, 84. (d) Fonseca-Guerra, C.; Visser, O.; Snijders, J. G.; te Velde, G.; Baerends, E. J. In *Methods and Techniques in Computational Chemistry: METECC-95*; Clementi, E., Corongiu, G., Eds.; STEF: Cagliari, Italy, 1995; pp 305−395.

(21) (a) Snijders, J. G.; Baerends, E. J.; Vernooijs, P. *At. Data Nucl. Data Tables* **1982**, *26*, 483. (b) Vernooijs, P.; Snijders, J. G.; Baerends, E. J. *Slater type basis functions for the whole periodic system;* Internal Report, Free University of Amsterdam: Amsterdam, The Netherlands, 1981.

(22) Frisch, M. J.; Trucks, G. W.; Schlegel, H. B.; Scuseria, G. E.; Robb, M. A.; Cheeseman, J. R.; Zakrzewski, V. G.; Montgomery, J. A., Jr.; Stratmann, R. E.; Burant, J. C.; Dapprich, S.; Millam, J. M.; Daniels, A. D.; Kudin, K. N.; Strain, M. C.; Farkas, O.; Tomasi, J.; Barone, V.; Cossi, M.; Cammi, R.; Mennucci, B.; Pomelli, C.; Adamo, C.; Clifford, S.; Ochterski, J.; Petersson, G. A.; Ayala, P. Y.; Cui, Q.; Morokuma, K.; Malick, D. K.; Rabuck, A. D.; Raghavachari, K.; Foresman, J. B.; Cioslowski, J.; Ortiz, J. V.; Stefanov, B. B.; Liu, G.; Liashenko, A.; Piskorz, P.; Komaromi, I.; Gomperts, R.; Martin, R. L.; Fox, D. J.; Keith, T.; Al-Laham, M. A.; Peng, C. Y.; Nanayakkara, A.; Gonzalez, C.; Challacombe, M.; Gill, P. M. W.; Johnson, B. G.; Chen, W.; Wong, M. W.; Andres, J. L.; Head-Gordon, M.; Replogle, E. S.; Pople, J. A. *Gaussian 98*, revision A.6; Gaussian, Inc.: Pittsburgh, PA, 1998.

(23) Ginsberg, A. P. *J. Am. Chem. Soc.* **1980**, *102*, 111.

(24) (a) Noodleman, L. *J. Chem. Phys.* **1981**, *74*, 5737. (b) Noodleman, L.; Baerends, E. J. *J. Am. Chem. Soc.* **1984**, *106*, 2316. (c) Noodleman, L.; Norman, J. G.; Osborne, J. H.; Aizman, A.; Case, D. A. *J. Am. Chem. Soc.* **1985**, *107*, 3418. (d) Noodleman, L.; Davidson, E. R. *Chem. Phys.* **1986**, *109*, 131. (e) Noodleman, L.; Case, D. A.; Aizman, A. *J. Am. Chem. Soc.* **1988**, *110*, 1001.

(25) (a) Bencini, A.; Totti, F.; Daul, C. A.; Doclo, K.; Fantucci, P.; Barone, V. *Inorg. Chem.* **1997**, *36*, 5022. (b) Ruiz, E.; Cano, J.; Alvarez, S.; Alemany, P. *J. Comput. Chem.* **1999**, *20*, 1391.

(26) (a) Ruiz, E.; Alemany, P.; Alvarez, S.; Cano, J. *J. Am. Chem. Soc.* **1997**, *119*, 1297. (b) Illas, F.; Moreira, I. de P. R.; de Graaf, C.; Barone, V. *J. Phys. Chem.* **1997**, *101*, 1526. (c) Cano, J.; Alemany, P.; Alvarez, S.; Verdaguer, M.; Ruiz, E. *Chem. Eur. J.* **1998**, *4*, 476. (d) Lledós, A.; Moreno-Mañas, M.; Sodupe, M.; Vallribera, A.; Mata, I.; Martínez, B.; Molins, E. *Eur. J. Inorg. Chem.* **2003**, 4187.

(27) (a) Petrie, S.; Stranger, R. *Inorg. Chem.* **2002**, *41*, 2341. (b) Stranger, R.; Petrie, S. *J. Chem. Soc., Dalton Trans.* **2002**, 1163. (c) Petrie, S.; Stranger, R. *Polyhedron* **2002**, *21*, 1163 and references therein. (d) Delfs, C. D.; Stranger, R. *Inorg. Chem.* **2001**, *40*, 3061 and references therein.

(28) Duclusaud, H.; Borshch, S. A. *J. Am. Chem. Soc.* **2001**, *123*, 2825.

(29) (a) Blasco, S.; Demachy, I.; Jean, Y.; Lledós, A. *New J. Chem.* **2002**, *26*, 1118. (b) Blasco, S.; Demachy, I.; Jean, Y.; Lledós, A. *Inorg. Chim. Acta* **2000**, *300−302*, 837. (c) Demachy, I.; Lledós, A.; Jean, Y. *Inorg. Chem.* **1999**, *38*, 5443. (d) Demachy, I.; Jean, Y.; Lledós, A. *Chem. Phys. Lett.* **1999**, *303*, 621. (e) Lledós, A.; Jean, Y. *Chem. Phys. Lett.* **1998**, *287*, 243.

(30) (a) Dirac, P. A. M. *Proc. R. Soc. London, Ser. A* **1926**, *112*, 661; **1929**, *123*, 714. (b) Heisenberg, W. *Z. Phys.* **1926**, *38*, 411. (c) van Vleck, J. H. *Theory of Electric and Magnetic Susceptibilities*; Oxford University Press: London, 1932.

(31) (a) Caballol, R.; Castell, O.; Illas, F.; Moreira, I. de P. R.; Malrieu, J. P. *J. Phys. Chem.* **1997**, *101*, 7860. (b) Cabrero, J.; Calzado, C. J.; Maynau, D.; Caballol, R.; Malrieu, J. P. *J. Phys. Chem. A* **2002**, *106*, 8146.

(32) (a) Yamaguchi, K.; Takahara, Y.; Fueno, T.; Nasu, K. *Jpn. J. Appl. Phys.* **1987**, *26*, L1362. (b) Onishi, T.; Soda, T.; Kitagawa, Y.; Takano, Y.; Daisuke, Y.; Takamizawa, S.; Yoshioka, Y.; Yamaguchi, K. *Mol. Cryst. Liq. Cryst.* **2000**, *143*, 133. (c) Onishi, T.; Takano, Y.; Kitagawa, Y.; Kawakami, T.; Yoshioka, Y.; Yamaguchi, K. *Polyhedron* **2001**, *20*, 1177.

(33) Cotton, F. A.; Walton, R. A. *Multiple Bonds Between Metal Atoms*; Wiley-Interscience: New York, 1982.

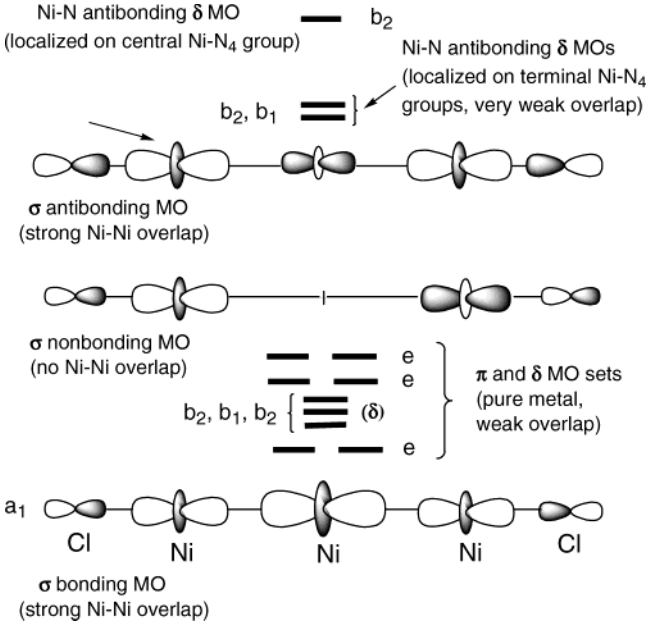

Figure 2. Sequence of the nickel framework MOs adapted to the D_4 point group obtained from DFT calculations on the high-spin ($^5A_1$) state of $Ni_3(dpa)_4Cl_2$. The notation $Ni-N_4$ designates a nickel atom together with its equatorial environment of four nitrogens.

character (a_1, a_2, and a_1 symmetry, respectively) are represented in Figure 2. At a Ni−Ni distance of ∼2.4 Å, the d_{z^2} orbitals develop an important overlap giving rise to a large energy splitting between the three combinations. Furthermore, it should be noted that all three σ combinations are pushed up in energy due to an antibonding interaction with the axial chlorine ligands (Figure 2).

In accordance with the standard ligand-field theory, a similar metal−ligand antibonding interaction occurs between the equatorial ligands and the properly oriented metal δ-orbital combinations. As a consequence of the helical shape of polypyridylamide ligands, these antibonding counterparts to the orbitals describing the dpa → nickel donation are *not* facing each other along the chain of metal atoms, and their overlap can be considered as negligible. Within the delocalized orbital model, they give rise to MO combinations belonging to the b_1 and b_2 representations of D_4, that will be denoted δ_{Ni-N^*}. These three δ_{Ni-N^*} MOs do not show up in the same energy region. Since the central nitrogen of the dpa ligand, which is the site of deprotonation, is significantly more basic than the pyridinic coordination sites,[14] the interaction with the metal is stronger, and the antibonding counterpart to this interaction is found at higher energies. The corresponding MO (b_2 symmetry) has practically all of its weight coming from the *central* $Ni-N_4$ system and can be considered as localized on this site. The two δ_{Ni-N^*} MOs involving the terminal sites appear lower in energy, namely, in the same energy region as the σ^* orbital of the metal framework (Figure 2). They are quasi-degenerate and do not show any significant contribution from the central site. Because of the energy competition between the σ^* orbital and the two $\delta_{Ni(terminal)-N^*}$ MOs, the interplay between the interactions involving the *axial* and the *equatorial* ligands will induce a variability of the electronic structure of the $[Ni_3(dpa)_4]^{q+}$ framework as a function of (i) the oxidation state and (ii) the strength of the axial donation.

In practice, the σ-bonding orbital, lowest in energy, and the nine orbitals of the π/δ block with pure metal character (Figure 2) are doubly occupied in all trinickel systems discussed in the present study. At the other end of the energy scale, the most destabilized $\delta_{Ni(central)-N^*}$ orbital remains empty in all states of interest. In between, the four metal electrons remaining to be accommodated will be distributed among (i) the σ_{nb} orbital; (ii) the σ^* orbital, and (iii) the two $\delta_{Ni(terminal)-N^*}$ orbitals (Figure 2). The nature of the electronic ground state and the associated structural features will depend upon this distribution. The critical property of *electrical conduction* will also depend on this distribution, and more specifically on the distribution of electrons *in the set of delocalized MOs with σ character, namely, σ, σ$_{nb}$, and σ**. As a matter of fact, the two $\delta_{Ni(terminal)-N^*}$ MOs are quasi-degenerate as a consequence of the near-zero overlap between the atomic δ orbitals. These symmetry-adapted combinations are therefore physically equivalent to *localized orbitals* centered on both ends of the metal framework. By contrast, the σ orbitals are the only ones to be physically, and not only mathematically, delocalized, due to the large σ overlap occurring between adjacent Ni atoms. Therefore, the existence of a localized electronic state is conditioned by the requirement of a double occupancy for all three metal orbitals with σ character. The occurrence of such a $(\sigma)^2(\sigma_{nb})^2(\sigma^*)^2$ ground state, diamagnetic and with no metal−metal interaction, has been discussed by Cotton et al. and tentatively ruled out for **1**,[12] since it does not fit the magnetic measurements. On the opposite, this diamagnetic state was advocated to be the ground state of $[Ni_3(BPAP)_4]^{2-}$ (with $HBPAP^- = 2,6$-bis(phenylamino)pyridine), a $(Ni_3)^{6+}$ complex devoid of axial ligand.[34] It is clear that any organization of the valence electrons different from $(\sigma)^2(\sigma_{nb})^2(\sigma^*)^2$ entails a partial or total depopulation of the σ^* orbital, and therefore implies at least *some* Ni−Ni−Ni delocalized bonding character and an enhanced probability to observe long-distance electrical conduction.[11]

The Superexchange Interaction in $Ni_3(dpa)_4Cl_2$ and Higher Homologues

The magnetic data reported for **1** and their fit by a simple dimer model using the HDVV Hamiltonian[30] are consistent with an antiferromagnetic interaction between the terminal nickel atoms of the complex, considered as high-spin Ni^{II} ions.[12−15] The value of the coupling constant deduced by Cotton's group from the HDVV model was $2J_{13} = -216$ cm^{-1} (see note 18 in ref 15). A similar fit carried out on the pentanickel homologue $Ni_5(tpda)_4Cl_2$ is interpreted by means of a similar coupling between terminal Ni atoms and yields $2J_{15} = -33.5$ cm^{-1}.[17] The same interpretation was proposed by Peng's group for the whole sequence of presently available $Ni_{2n+3}(polypyridylamide)_4Cl_2$ with $2J$ values decreasing from -198 cm^{-1} for **1** to -3.4 cm^{-1} for $Ni_9(peptea)_4Cl_2$.[2] It

(34) Cotton, F. A.; Daniels, L. M.; Lei, P.; Murillo, C. A.; Wang, X. *Inorg. Chem.* **2001**, *40*, 2778.

Table 1. Properties[a] Calculated in the Quintet, Antiferromagnetic Singlet (Approximated by the Broken-Symmetry Solution), and Diamagnetic Singlet States of $Ni_3(dpa)_4Cl_2$ Using Different Exchange-Correlation Functionals and Atomic Basis Sets[b]

	high-spin state				antiferromagnetic state (BS)			low-spin state (diamagnetic)[c]			exptl[d]	
	S/II	S/IV	G/I	G/II	S/II	G/I	G/II	S/II	G/I	G/II	$Ni_3(dpa)_4Cl_2$	$[Ni_3(BPAP)_4]^{2-}$
distances												
Ni−Ni	2.439	2.442	2.457	2.462	2.415	2.452	2.454	2.386	2.381	2.388	2.42−2.44	2.368
Ni−Cl	2.410	2.355	2.453	2.397	2.418	2.454	2.397	2.58	3.04	2.92	2.325−2.34	
$Ni_{term.}$−N	2.086	2.104	2.102	2.117	2.080	2.100	2.115	2.009	1.954	1.965	2.08−2.10	1.90−1.91
Ni_{center}−N	1.897	1.916	1.914	1.913	1.895	1.914	1.913	1.893	1.910	1.905	1.88−1.89	1.92
spin distribution												
$Ni_{term.}$	+1.37	+1.36	+1.59	+1.57	±1.29	±1.59	±1.58					
Ni_{center}	+0.25	+0.24	+0.11	+0.11	0.0	0.0	0.0					
Cl	+0.15	+0.14	+0.09	+0.10	±0.13	±0.09	±0.095					
$N_{term.}$	+0.08	+0.08	+0.07	+0.07	±0.075	±0.06	±0.06					
N_{center}	+0.02	+0.02	+0.01	+0.01	0.0	0.0	0.0					
$\langle S^2 \rangle$			6.013	6.014		1.992	1.993					
$-2J$ (cm^{-1})					645	110	91				216 198[e]	
ΔE (kcal·mol^{-1})	+3.69		+0.63	+0.52	0.	0.	0.	+16.0	+23.8	+30.8		

[a] Selected interatomic distances (Å), atomic spin distribution (electrons), antiferromagnetic coupling constant (cm^{-1}), $\langle S^2 \rangle$ eigenvalues (dimensionless), relative energies ΔE of the considered states (kcal·mol^{-1}). [b] S/II: BP86 functional, valence double-ζ Slater basis sets. S/IV: BP86 functional, valence triple-ζ Slater + polarization basis sets. G/I: B3LYP functional, LANL2DZ Gaussian basis set for Ni, Cl, N. G/II: LANL2DZ + polarization Gaussian basis set for Ni, Cl, N (see Computational Details). [c] Corresponds to the electronic configuration $(\sigma)^2(\sigma_{nb})^2(\sigma^*)^2$. [d] For $Ni_3(dpa)_4Cl_2$, taken from ref 12, unless explicitly specified; for $[Ni_3(BPAP)_4]^{2-}$, taken from ref 34. [e] Reference 2.

is assumed in this model that the metal atoms not occupying a terminal position are *not* active magnetic centers.

DFT calculations, carried out either with the GGA/BP86 or with the hybrid B3LYP functional, confirm the antiferromagnetically coupled model as the ground state of **1** (Table 1). The calculated values of the coupling constant are however strongly dependent upon the selected functional. B3LYP calculations with basis set G/I yield an energy difference of 0.63 kcal·mol^{-1} between the broken-symmetry (BS) solution at equilibrium and the high-spin, quintet state. The value of ${}^{BS}\langle S^2 \rangle$ was calculated to be 1.99, that is, close to $S_{max} = 2$ and indicative of a low overlap between the magnetic orbitals. The application of eq 2 therefore yields an estimate of 110 cm^{-1} for $-2J_{13}$. Adding polarization functions (basis set G/II) slightly decreases this value to 91 cm^{-1}. Assuming the same negligible overlap between the magnetic orbitals, the GGA functional yields a much higher value for the coupling constant (645 cm^{-1}). Similar, though less important, discrepancies have been documented in the case of coupled dicopper species and were interpreted in terms of a systematic overestimation of the (${}^{BS}E - {}^{HS}E$) gap by the GGA functional, due to an excessive delocalization of the magnetic orbitals.[31,32] The contributions of the spin-polarized orbitals to the nonmagnetic metal exactly cancel each other in the BS solution, but are additive in the quintet state. The atomic spin value calculated at $Ni_{central}$ in the ${}^5A_1$ state therefore provides an estimate to the tendency of the spin-polarized electrons to spread over the whole molecule. In a purely localized model, this atomic spin value should be very close to zero. In fact, the GGA functional yields a large spin delocalization, with an integrated value of 0.25e on the central nickel (Table 1). This value is reduced to 0.11e with the hybrid B3LYP functional, still indicative of a significant overlap. In view of the values obtained for $-2J_{13}$, real delocalization should be in between, and relatively close to the B3LYP results.[35]

This antiferromagnetic state of polynickel wires was described by Cotton et al. in terms of a coupling between two terminal Ni^{II} atoms in the high-spin ($S = 1$) state separated by one or several Ni^{II} atoms in the low-spin ($S = 0$) state.[12−15] This description was recently refined by Berry et al., who suggest a superexchange mechanism coupling the terminal nickel atoms through $Ni_{central}$. The role of the central nickel is substantiated by a correlation between the variation of the Ni−Ni distances observed in a series of $Ni_3(dpa)_4L_2$ compounds and the magnitude of the antiferromagnetic coupling.[36] The interpretation based on DFT calculations corroborates the mechanism proposed on experimental grounds: the high-spin state of the terminal nickel atoms is induced by the relatively weak donor strength of the pyridine nitrogens, allowing one metal electron pair to be distributed between the d_{z^2} orbital and the high-lying $\delta_{Ni(term.)-N^*}$ orbital. As discussed above, this latter electron can be considered as remaining localized on the terminal Ni atom and its equatorial environment. At variance with that, the electron accommodated on d_{z^2} is assigned to the pool of σ electrons and delocalized. As far as the central nickel is concerned, its localized δ_{Ni-N^*} orbital is too high in energy to be accessible. The electronic configuration of $Ni_{central}$ is therefore basically closed-shell, and two of its electrons are assigned to the set of σ orbitals.[36] As inferred from the low value observed and computed for the coupling constant $-2J$, the antiferromagnetic ground state is in close competition with a high-spin quintet state, which is properly described in terms of delocalized orbitals by a single electronic configuration. The magnetic orbitals in this configuration and their symmetry in the D_4 point group are as follows: (i) σ_{nb} (a_2); (ii) σ^* (a_1); (iii) $\delta_{Ni(1)-N^*} + \delta_{Ni(p)-N^*}$ (b_2); (iv) $\delta_{Ni(1)-N^*}$

(35) In the high-spin quartet state of the oxidized complex, in which σ^* is unoccupied, the spin at Ni_{center} becomes slightly negative (Table 2).

(36) Berry, J. F.; Cotton, F. A.; Murillo, C. A. *J. Chem. Soc., Dalton Trans.* **2003**, 3015.

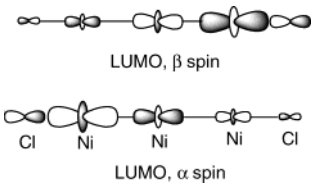

Figure 3. Degenerate spin-polarized LUMOs obtained from the broken-symmetry DFT approach of the antiferromagnetic ground state of $Ni_3(dpa)_4Cl_2$.

$-\ \delta_{Ni(p)-N^*}$ (b_1). The double occupancy of the low-lying σ orbital, incompletely balanced by the single occupancy of the delocalized σ^* orbital, implies some bonding all along the linear metal framework, extending to the axial chlorines through the $Ni_{(term.)}-Cl$ interaction (Figure 2). The reality of the antiferromagnetic ground state might seem more difficult to capture, since the broken-symmetry solution used to estimate its relative energy is not a physical state.[24,31,32] The physical significance of the optimal geometry and of the magnetic orbitals stemming from the unprojected BS solution is, however, admitted.[26−28] In the present case, the BS optimal geometries do not significantly differ from those of the quintet state (Table 1), which means that bonding interactions are little affected by the spin coupling. This is confirmed by the nature of the spin-polarized LUMOs, which retain an important metal−metal and metal−chlorine σ^* character (Figure 3).

Electronic and Structural Variability of Trinickel Complexes

Structure of Neutral $Ni_3(dpa)_4Cl_2$. The molecular geometry of **1** in the antiferromagnetic singlet ground state (as approximated by the broken-symmetry solution), in the diamagnetic singlet state, and in the high-spin quintet state has been optimized with both the GGA/BP86 and the B3LYP functionals and with various basis sets. Selected interatomic distances and atomic spin values are displayed in Table 1. Observed distances are quite closely reproduced at all levels of calculation, with the exception of the Ni−Cl bond lengths, overestimated by ∼0.1 Å with the nonpolarized basis sets. Inclusion of polarization functions reduces this discrepancy without affecting the other bond lengths (Table 1). Distances calculated with a given basis set for the quintet state and for the antiferromagnetic singlet differ by less than 0.03 Å. The electronic reorganization to the diamagnetic singlet state implies a two-electron transfer from the two $\delta_{Ni(term.)-N^*}$ orbitals to the upper metal σ combinations, yielding the $(\sigma)^2(\sigma_{nb})^2(\sigma^*)^2$ configuration. The energy cost of this electronic reorganization was calculated to be 16.0 kcal·mol^{-1} with the GGA functional, and 23.8 kcal·mol^{-1} with B3LYP/G/I. This energy difference tends to increase when polarization functions are added (Table 1). It has been mentioned above that this electronic state corresponds to a localized, globally nonbonding description of the metallic framework. It is also characterized by very important changes in the molecular geometry. The first structural consequence of the full occupancy of σ_{nb} and σ^* is a dramatic elongation of the Ni−Cl distances. The distances calculated with B3LYP are of the order of 3.0 Å (Table 1), which can be assimilated to

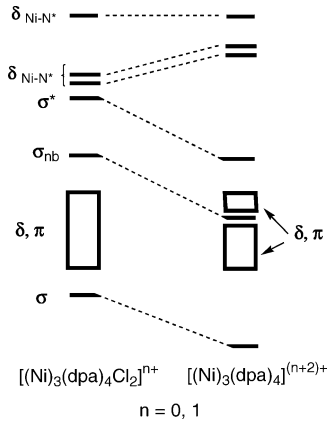

Figure 4. Orbital diagram showing the effect of a removal of the axial chlorine ligands in trinickel complexes.

a dissociative trend, easily explained by the strong Ni−Cl antibonding character of the upper σ combinations (Figure 2).[37] The other structural effect that can be expected from the depopulation of the $\delta_{Ni(term.)-N^*}$ orbitals is a contraction of the $Ni_{terminal}-N$ distances. Such a contraction is indeed obtained from the calculations and amounts to 0.15 Å with B3LYP (Table 1).[37] The $Ni_{term.}-N$ distances in the diamagnetic singlet, however, remain longer than the $Ni_{center}-N$ ones by 0.045 to 0.06 Å (with B3LYP),[37] which illustrates the effect of the difference in basicity between the two types of N ligands. A more unexpected structural consequence of the change from an antiferromagnetic to a diamagnetic state is a *contraction* of the Ni−Ni bond length, by ∼0.06 Å (Table 1).[37] The opposite could have been expected with regard to the shift from a partly bonding to a nonbonding metal−metal electronic configuration. In fact, two factors tend to counteract the trend toward an expansion of the Ni−Ni distance. First is the vanishing of the trans influence exerted by the axial ligands. The lengthening of the Ni−Ni distance assigned to the trans effect can be estimated to be 0.06/0.08 Å from the calculations. The second factor is the important transfer of electronic density toward the region of the trimetallic axis, which efficiently shields the electrostatic repulsion between the positively charged nickel atoms. It should finally be noted that, in spite of its high relative energy, the diamagnetic singlet really represents an energy minimum on the potential energy hypersurface. This is a consequence of the stabilization of all three σ orbitals of $(Ni_3)^{6+}$ induced by the loss of axial coordination (Figure 4). Furthermore, the depopulation of the $\delta_{Ni(term.)-N^*}$ orbitals moves these MOs to higher energies as a consequence of the Ni−N bond contraction, thus widening the HOMO−LUMO gap (Figure 4). This effect confers the diamagnetic singlet the status of a high-energy metastable state. The replacement of the dpa ligands by the bulky BPAP anions, which impede axial coordination, has led to the characteriza-

(37) The structural changes associated with the diamagnetic singlet state follow the same trend when calculated with the BP86 functional, but they are significantly less dramatic: the Ni−Cl distance is stabilized at 2.58 Å; the contraction of the $Ni_{term.}-N$ bond length is limited to 0.07 Å and that of Ni−Ni to 0.03 Å (Table 1). This should be assigned to the well-documented trend toward orbital overdelocalization induced by pure GGA functionals which tends to smooth the description of "catastrophic" events such as bond-breaking.

Table 2. Selected Properties[a] Calculated for the Doublet Ground State of $[Ni_3(dpa)_4]^{3+}$ and for the Lowest Doublet and Quartet States of $[Ni_3(dpa)_4Cl_2]^{+}$ with the GGA/BP86 Functional and Two Different Atomic Basis Sets

	$[Ni_3(dpa)_4Cl_2]^+$				$[Ni_3(dpa)_4]^{3+}$		
	doublet state		quartet state		doublet state		
	S/II	S/IV	S/II	S/IV	S/II	S/IV	exptl[b]
distances							
Ni−Ni	2.357	2.377	2.378	2.378	2.294	2.295	2.285/2.289
Ni−Cl	2.430	2.520	2.335	2.292			
$Ni_{term.}$−N	2.019	1.981	2.076	2.088	1.944	1.959	1.929
Ni_{center}−N	1.885	1.888	1.890	1.913	1.878	1.891	1.881
spin distribution							
$Ni_{term.}$	+0.27	+0.26	+1.00	+0.94	+0.29	+0.28	
Ni_{center}	+0.24	+0.26	-0.08	-0.08	+0.39	+0.39	
Cl	+0.09	+0.08	+0.07	+0.06			
$N_{term.}$	+0.003	+0.004	+0.09	+0.08	+0.001	+0.002	
N_{center}	+0.003	+0.005	+0.05	+0.06	+0.005	+0.005	
ΔE (kcal·mol^{-1})	0.	0.	+10.9	+11.7			

[a] Interatomic distances (Å), atomic spin distribution (electrons), and relative energies ΔE (kcal·mol^{-1}). [b] From ref 15.

tion of a linear complex of $(Ni_3)^{6+}$ displaying the structural and magnetic signature of the diamagnetic singlet state.[34] It could be noted that the Ni−Ni distance observed in $[Ni_3(BPAP)_4]^{2-}$ is shorter than that of **1** by 0.05/0.07 Å, in agreement with the structural trends calculated for the *diamagnetic state* of **1** (Table 1).

Oxidized Trinickel Complexes: $[Ni_3(dpa)_4Cl_2]^+$ ($\mathbf{1}^+$) and $[Ni_3(dpa)_4]^{3+}$ (2). The effect of a one-electron oxidation on the electronic and structural configurations of the trinickel species has been investigated by means of calculations carried out on $\mathbf{1}^+$ and **2** with the BP86 functional and the two basis sets S/II and S/IV. For $\mathbf{1}^+$, a low-spin ($^2A_1$) and a high-spin ($^4A_1$) electronic state have been investigated and their geometries optimized by means of unrestricted, symmetry-adapted calculations. The quartet state of **2** is expected to be very high in energy and has not been investigated. The most important geometrical parameters and the atomic spin distribution are displayed in Table 2. **2** has been synthesized and its structure characterized from X-ray diffraction.[15] It is not coordinated in axial position, except for relatively long range interactions with two $(PF_6)^-$ counterions. The structure of this complex is especially intriguing because of a remarkable contraction of the coordination sphere around the terminal nickels, associated with a dramatic change of the electronic state of terminal nickel atoms from high spin to low spin. The decrease of the Ni−Ni distance from ∼2.44 Å in **1** to 2.285 Å in **2** has been highlighted and assigned to the setting up of delocalized Ni−Ni bonding.[13−15] However, less attention has been paid to the equivalent shortening of the $Ni_{term.}$−N distances. Let us refer to the ground state of **1** and to the closely related quintet state, with two of its magnetic orbitals displaying $Ni_{term.}$−N antibonding character. On the one hand, the observed contraction of the $Ni_{term.}$−N distances should be assigned to the depopulation of these latter MOs. On the other hand, no modification of the Ni_{center}−N distances is observed, which means that the corresponding $\delta_{Ni(center)-N^*}$ orbital remains empty. Following the orbital scheme of Figure 2, the only electronic configuration available to **2** should be $(\sigma)^2(\sigma_{nb})^2(\sigma^*)^1$. The calculations indeed found the corresponding $^2A_1$ state lowest in energy. In terms of delocalized bonding, this configuration only differs from that of **1** by the accommodation of one more electron on the nonbonding σ MO, which has no contribution on Ni_{center} (Figure 2). How can such an electronic arrangement induce the shrinkage of the Ni−Ni distance? The question has already been briefly discussed in the above section. Part of the contraction should be assigned to the vanishing of the trans influence of the axial ligands. Letting axial chlorines approach the oxidized species to yield $\mathbf{1}^+$ is sufficient to stretch the metal−metal distance from 2.295 to 2.377 Å (Table 2). The recent structural characterization of a series of $Ni_3(dpa)_4L_2$ compounds with various axial ligands has indeed established that modifying the donor strength of L induces variations of the Ni−Ni distance with the same order of magnitude.[36] The other effect is electrostatic and results from the efficient shielding of the positive charge stemming from the $(Ni_3)^{7+}$ backbone by an increased electron density gathered along the σ axis. One may even argue that the extra positive charge introduced in the metal framework by oxidation represents the incentive toward the change of the electronic configuration. The quartet state $^4A_1$ which corresponds to the $(\sigma)^2(\sigma_{nb})^1(\sigma^*)^0$ configuration and retains two electrons accommodated in the $\delta_{Ni(term.)-N^*}$ orbitals was found higher in energy (+11.7 kcal·mol^{-1}, Table 2). Indeed, this configuration yields a *deshielding* of the metal charge and is destabilized in the oxidized species.

The shielding effect induced by σ electron density and its influence on the metal−metal bond length clearly question the status of the σ nonbonding orbital. Because of its null weight on the central atom, this orbital is classically considered as *neither bonding nor antibonding*. In spite of a zero contribution to the formal bond order and to electron delocalization, the σ_{nb} orbital is not quite innocent, since its population influences the bond length as a function of the net charge of the atomic triad. One could therefore assign this orbital a more dynamic and versatile role by telling that it is *either bonding or antibonding*, depending on the sign of the atomic net charges. According to this tentative definition, the population of σ_{nb} in linear $(M_3)^{6+}$ species should be assigned a bonding influence, still enhanced upon oxidation of the metal framework to $(M_3)^{7+}$

Extrapolation to Nickel Wires with Higher Nuclearity

The assignment of the electronic configuration of $(Ni_3)^{6/7+}$ complexes, associated with a pretty good modeling of their observed structure, has important consequences regarding the possible ability of these systems, and of more extended compounds of the same type, to initiate, tune, or control the transit of electrons through a nanocircuit.[17] Here, we show that, in spite of important structural discrepancies between **1** and its oxidized, axially free counterpart **2**, the shape and the occupancy of the two molecular orbitals responsible for the delocalized bonding along the metal framework, namely, the bonding σ and the antibonding σ^* MOs, are not modified upon ionization. The change in the electronic structure, however, affects the population of a third combination of metal d_{z^2} orbitals, referred to as σ_{nb}. This MO belongs to the

a_2 representation of the D_4 group; it is antisymmetric with respect to the C'_2 and C''_2 rotation axes, and its contribution to the central Ni atom is therefore strictly zero: σ_{nb} is basically *localized* on separate parts of the chain, even though its population is expected to yield a contraction of the metal−metal distances along the chain. The electronic configuration of the $(Ni_3)^{6/7+}$ complexes of dpa can be written as $(\sigma)^2(\sigma_{nb})^q(\sigma^*)^1$ with $q = 1$ for the neutral species and $q = 2$ for the oxidized complex. *Due to the relatively large overlap between the metal d_{z^2} orbitals in the considered range of Ni−Ni distances, the delocalization issue is conditioned by the population of the σ* orbital. An incomplete population of σ*, in the standard as in the oxidized forms, provides all $(Ni_3)^{6/7+}$ complexes with some delocalized metal−metal bonding*.

The structural and magnetic data reported by Peng's group for a series of four neutral nickel wires with increasing number of metal atoms ranging from $Ni_3(dpa)_4Cl_2$ to the nonanickel homologue $Ni_9(peptea)_4Cl_2$ suggest that the conclusions obtained from the investigation of the trinickel complex can be extended to higher nuclearity compounds.[2] All compounds investigated by Peng are antiferromagnetic, with regularly decreasing values of $-2J$. Furthermore, in all four complexes, the observed $Ni_{term.}$−N distances are stretched by ∼0.2 Å with respect to the other, internal Ni−N distances, all ranging between 1.89 and 1.93 Å.[2] These structural and magnetic data strongly support the idea of an electronic activation of the terminal nickel atoms similar to that observed for **1**, with the transfer of one electron into each $\delta_{Ni(term.)-N^*}$ localized orbital. Two metal electrons will therefore be missing to complete the double occupancy of the whole set of p σ-type orbitals obtained from appropriate delocalized combinations of the p d_{z^2} atomic orbitals. At that point, two possibilities are left open for the electronic configuration of the high-spin counterpart to the antiferromagnetic ground state. These two configurations differ in the electron occupancies in the set of σ-type orbitals, labeled in accordance with the aufbau sequence:

$$(\sigma_1)^2...(\sigma_{p-2})^2(\sigma_{p-1})^2(\sigma_p)^0 \quad (3)$$

or

$$(\sigma_1)^2...(\sigma_{p-2})^2(\sigma_{p-1})^1(\sigma_p)^1 \quad (4)$$

σ_p therefore denotes the σ MO highest in energy, with fully antibonding character and a_1 symmetry, whereas σ_{p-1} is an orbital with a_2 symmetry and zero contribution to the central metal atom.[38] Accounting for the two singly occupied $\delta_{Ni(term.)-N^*}$ orbitals, configuration 4 is associated with a $^5A_1$ high-spin state analogous to the one discussed for **1**. Configuration 3 would be associated with a triplet state, with two $\delta_{Ni(term.)-N^*}$ magnetic orbitals. An antiferromagnetic coupling of the electrons accommodated in these orbitals should occur exclusively through the equatorial ligands and yield a brutal collapse of the magnetic coupling constant. Since the value of $-2J$ just smoothly decreases when the metal chain is extended,[2] the hypothesis of a change in the electronic configuration can be tentatively ruled out.

The crystal structure of the oxidized complex $[Ni_5(etpda)_4]^{3+}$ (etpda = the anion of *N*,*N*′-bis(4-ethylpyridyl)-2,6-diaminopyridine) has been resolved by Cotton's group.[17] The evolution of the Ni−N and of the Ni−Ni distances with respect to the neutral complex closely parallels the contraction observed for $[Ni_3(dpa)_4]^{3+}$. An important point is that the contraction of the metal framework not only affects the most external Ni−Ni bonds but also extends to *all* four metal−metal distances.[17] Assuming that the shortening of the Ni−Ni bonds could be partly assigned, as for **2**, to a more efficient shielding of the metal positive charge along the σ axis, the observed contraction could be explained by the transfer of one electron from the δ orbitals to the σ_4 MO, which extends over all Ni atoms but the central one.[38]

To summarize, the magnetic and structural data presently available for the $(Ni_p)^{2p+}$ and for the $(Ni_p)^{(2p+1)+}$ complexes seem compatible with a straightforward extension of the electronic structures deduced from DFT calculations carried out on $Ni_3(dpa)_4Cl_2$ and on $[Ni_3(dpa)_4]^{3+}$. Both the neutral and the oxidized complexes should be characterized by the permanence of *some* delocalized bonding character along the metal framework due to an incomplete occupancy of the highest, delocalized, and fully antibonding σ orbital.

Acknowledgment. Calculations have been carried out in part at the Centre Universitaire et Régional de Ressources Informatiques (CURRI, Université Louis Pasteur, Strasbourg, France) and in part at the IDRIS computer center (CNRS, Orsay, France). It is a real pleasure to thank Prof. F. A Cotton and C. A. Murillo for excellent advice, and for communicating their most recent results.

Supporting Information Available: Complete list of Cartesian coordinates for $Ni_3(dpa)_4Cl_2$, $[Ni_3(dpa)_4Cl_2]^+$, and $[Ni_3(dpa)_4]^{3+}$ in the low-spin and in the high-spin states, as optimized with the various atomic basis sets considered in the present work. This material is available free of charge via the Internet at http://pubs.acs.org.

IC040011J

(38) A sketch illustrating the sequence of the atomic orbital combinations that can be expected for $M_5(tpda)_4L_2$ is displayed in Yeh et al.: Yeh, C.-Y.; Chou, C.-H.; Pan, K.-C.; Wang, C.-C.; Lee, G.-H.; Su, Y. O.; Peng, S. M. *J. Chem. Soc., Dalton Trans.* **2002**, 2670.